CHAPTER IV

NUCLEATION AND PLASTICIZATION DUAL FUNCTIONS OF MULTI-BRANCHED POLY(L-LACTIC ACID) (PLLA) FOR PLA

Thammanoon Khamsarn [a], Suwabun Chirachanchai [a,b,*]

[a)] *The Petroleum and Petrochemical College, Chulalongkorn University,* Bangkok, Thailand

[b)] *Center for Petroleum, Petrochemical, and Advanced Materials,* Bangkok, Thailand

* ***csuwabun@chula.ac.th***

4.1 Abstract

Poly(lactic acid) (PLA) is the most reliable biodegradable polymer due to the industrial scale production and the variety of the products in the market. However, PLA performs extremely slow crystallization in comparison to other commercial petroleum-based polymers such as polypropylene (PP), polyethylene (PE), (1/70 times of high density polyethylene (HDPE) and shows the glass transition temperature (T_g,) above room temperature (58 °C).This leads to the brittleness and the low impact resistance. For the past several years, the improvement of PLA by enhancing crystallization as well as plasticization via the uses of nucleating agents such as starch and talc, and the uses of poly(butylene succinate) (PBS), poly(butylene adipate-*co*-terephthalate) (PBAT), etc. have been previously reported. However, the phase separation is still the main problem. Here, we propose multi-branched polymers as a dual functions additive, i.e. nucleating agent and plasticizer for 200% PLA as- evidenced from the significant crystallization and the lowering of T_g without phase separation.

Keywords: Dual functions, Multi-branched PLLA, Multi-branched polyethylenimide, Poly(*L*-lactide), Nucleating agent, Plasticizer

4.2 Introduction

In recent years, biodegradable polymers are of interest because they are obtained from renewable resources and can be used as environmental friendly

materials. The most potential biodegradable polymer is poly(*L*-lactic acid) (PLLA) (Pillin *et al.*, 2006) since it can be biodegradable polymer obtained from a complete industrial scale production. Commercial PLA resin with the presence of D-lactide was invertigated, the structure become disordered whereas spherulite size and time for crystallization increases(Tsuji and Muramatsu, 2001). As PLA is a aliphatic polyester, PLA can be made in various types of products, such as films, sheets, plates, fibers, etc., through different processing techniques of film blowing, sheet casting, injection moulding, tray thermoforming, spun-bond fiber spinning, etc. It should be noted that PLLA has an extremely slow crystallization rate which leads to product brittleness, low impact resistance and time consuming production, in comparison with other commercial petrochemical-based polymers such as polyethylene (PE), polypropylene (PP) (Kim *et al.*, 2010). It should be note that Avrami crystallization rate constants (ka) of high-density polyethylene (HDPE) at 120 °C was 1.21 min^{-1} whereas ka of PLA was only 0.01573 min^{-1}, approximately 1/70 times of HDPE (Sobkowicz *et al.*, 2008; Suryanegara *et al.*, 2010).

The crystallization rate and free volume of PLA can be enhanced significantly by blending both nucleating agents and plasticizers. The several nucleating agents were reported in the past such as starch (Cai *et al.*, 2011), talc (Li and Huneault, 2007), and calcium carbonate ($CaCO_3$) (Suksut and Deeprasertkul, 2011). Meanwhile, many polyols were utilized as plasticizer such as Polyethylene glycol (PEG) (Hu *et al.*, 2003), and glycerol (Li and Huneault, 2011). The fact that the main disadvantage of those nucleating agents and plasticizers is the phase separation from PLLA. Basically, the crystallization of short chain polymers is more rapid than the longer ones. In order to accelerate crystallization completely in short time, the short chain PLLA is an attractive candidate. Here, we consider the short chain PLLA as nucleating agent for not only helical crystalline structure formation in a short time but also effective induction of co-crystallization with long chain PLA at the same time.

4.3 Experiment

4.3.1 Materials and Chemicals

Multi-branched polyethyleneimine (*m*PEI, MW 25,000 g mol^{-1}) was dried under vacuum at 80 °C for 3 hours before use. All chemicals (Sigma-Aldrich) were used without further purification. Tin(II) 2-ethylhexanoate ($Sn(Oct)_2$, 97% purity) was purchased from Sigma-Aldrich and used directly. L-lactide was kindly provided by PTT Public Company Limited. Commercial PLA (2002D) was purchased from Natureworks LLC.

4.3.2 Preparation of Multi-branched Polyethylenimide-co-poly(lactic acid)

Multi-branched polyethylenimide-co-poly(lactic acid) (*m*PEI-PLLA) was synthesized through ring-opening polymerization of *L*-lactide (L-LA) and polyethylenimide by using tin octoate $Sn(Oct)_2$ as a catalyst (Figure 4.1).

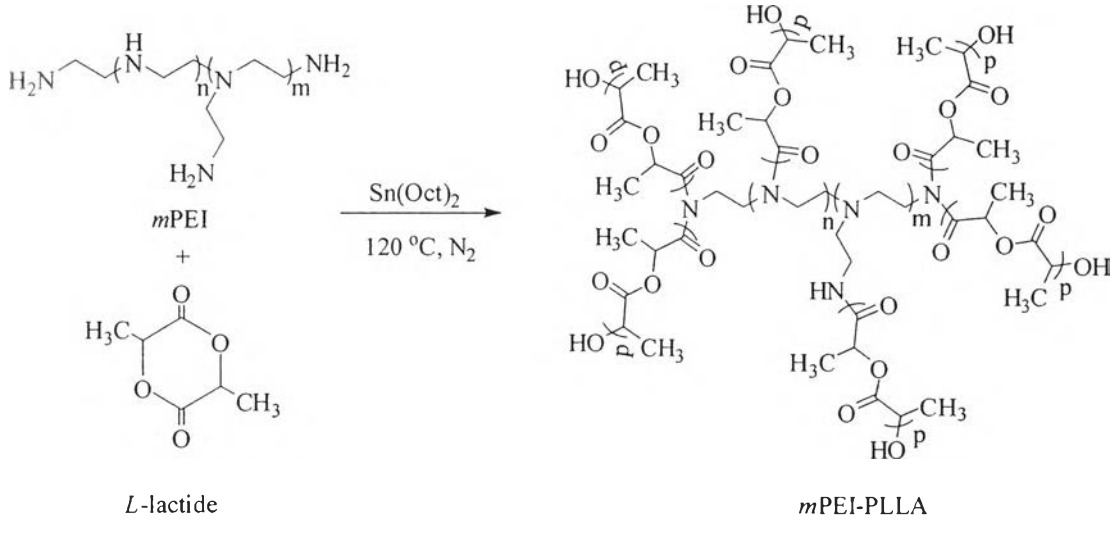

Figure 4.1 Preparation of *m*PEI-PLLAs.

The ring-opening polymerization was carried out at 120 °C for 4 h under nitrogen atmosphere. The product obtained was dissolved in chloroform and precipitated in diethyl ether before drying under vacuum at 60 °C for 24 h. The molar feed ratios of *m*PEI to L-lactide 1:166, 1:415, 1:830, 1:1162, 1:3320 and 1:6640 were used to obtain *m*PEI-$PLLA_3$, *m*PEI-$PLLA_5$, *m*PEI-$PLLA_{10}$, *m*PEI-$PLLA_{14}$, *m*PEI-$PLLA_{40}$ and *m*PEI-$PLLA_{80}$, respectively.

4.3.3 Preparation of PLA/*m*PEI-PLLA$_n$ Blend Films

Commercial PLA was blended with *m*PEI-PLLA by solution casting method. PLA (2002D commercial grade) (0.5 g) and *m*PEI-PLLAs (10, 20, and 30%) were dissolved in chloroform 15 ml. The solution was mixed under vigorous stirring for approximately 4 h. The solution was casted on petri-dish, and then the solvent was evaporated at room temperature for 48 h and further dried under vacuum for 48 h.

4.3.4 Characterization

4.3.4.1 Fourier Transform Infrared Spectroscopy (FTIR)

FTIR spectra were obtained from an FTIR spectrophotometer (Bruker EQUINOX 55) with 32 scans at a resolution of 4 cm^{-1} and wavenumber range of 4000 cm^{-1} to 400 cm^{-1}. The spectra were acquired and manipulated with OPUS software.

4.3.4.2 Nuclear Magnetic Resonance (NMR)

NMR spectra were obtained from a Bruker Ultrashield 500 Plus (500 MHz). The samples were dissolved in deuterated chloroform ($CDCl_3$).

4.3.4.3 Gel Permeation Chromatography (GPC)

Molecular weight and polydispersity were determined by a Shimadzu size-exclusion chromatograph (SEC) equipped (Polymer Laboratories, Varian Inc.) and a refractive index detector. Chloroform was used as an eluent at a flow rate of 1.0 mL min^{-1}. Polystyrene standards were used and the measurements were performed at 40 °C. The injection volume was 20 µL.

4.3.4.4 Differential Scanning Calorimeter (DSC)

Differential scanning calorimetry (DSC) measurement was performed on 5-10 mg samples under nitrogen atmosphere by using a NETZSCH-Proteus differential scanning calorimeter. Samples were heated from -70 to 200°C and then cooled to -70°C with 10°C/min. After that they were heated again to 200 at 5 °C/min (2^{nd} heating scan). Glass transition temperatures were measured from the inflection point in the 2^{nd} heating thermogram. Crystallization and melting enthalpies were determined from integral of their peaks.

4.3.4.5 Thermogravimetric Analysis (TGA)

Thermogravimetric analysis (TGA) technique was applied for 10-15 mg samples either under nitrogen atmosphere or under air with a Perkin Elmer Pyris Diamond. All samples were heated from 50 to 700 °C at 20 °C/min. Decomposition temperature at 5% weight loss (T_d) and the mass residue at 600 °C (WR 600) were measured in this study.

4.3.4.6 Scanning Electron Microscope (SEM)

Morphology of cross-section surface of film specimens was observed under a scanning electron microscope (SEM, Hitachi, S-4800). The samples were put on the holder with an adhesive tape and coated with a thin layer of platinum for 1 min.

4.3.4.7 Mechanical Properties

The mechanical properties of the PLA/*m*PEI-PLLA$_n$ blends films were investigated by a universal testing machine (Lloyd). The yield setup mode was used with preload of 0.1 N, a speed of 50 mm/min, and a gauge length of 50 mm. All films were under vacuum system before tensile test. The values of stress at break and elongation at break were reported. The sample was determined through different parameters (Chivrac *et al.*, 2006).

4.3.4.8 Crystallization Behavior

The crystallization behavior and spherulite morphology of PLA and PLA/*m*PEI-PLLA films were observed by a Leica DMRXP polarizing optical microscope (POM) equipped with a Mettler Toledo FP90 central processor hot stage. Each film was heated from 25 °C to 200 °C at 20 °C min^{-1} before kept at 200 °C for 2 min to allow complete melting, and then subjected to another hot stage at 110 °C to observe spherulite formation.

4.4 Results and discussion

4.4.1 Structural Characterization of *m*PEI-PLLA$_n$ Copolymers

The *m*PEI-PLLAs were synthesized by applying polyethylenimine (*m*PEI, M_n = 2.5×10^4 g mol^{-1}) as a macroinitiator and carrying out ring-opening polymerization of *L*-lactide using tin(II) 2-ethylhexanoate ($SnOct_2$) as a catalyst

(Figure 4.1). *m*PEI with $M_n = 2.5\times10^4$ g mol^{-1} (*m*PEI25K) has reactive groups around 166 units, containing 72 units of terminal end group primary amine, and 94 units of linear secondary amine, confirmed by quantitative analysis from ^{13}C-NMR (D_2O) in zgig mode (Pangon *et al.*, 2011). It was used as core molecules (Appendix A (Figure A1)).

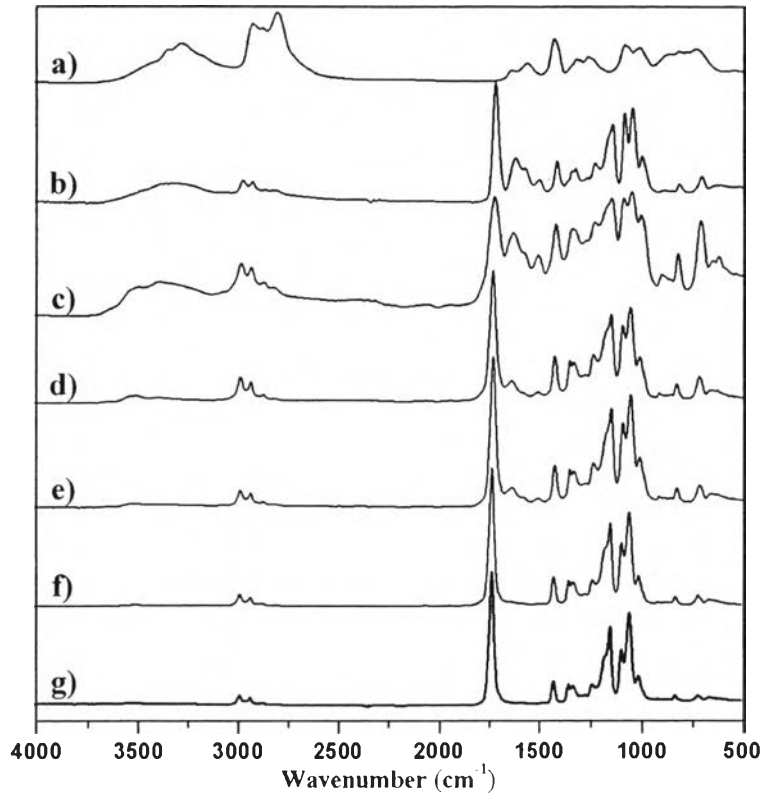

Figure 4.2 FTIR spectra of a) *m*PEI, b) *m*PEI-PLLA$_3$, c) *m*PEI-PLLA$_5$, d) *m*PEI-PLLA$_{10}$, e) *m*PEI-PLLA$_{14}$, f) *m*PEI-PLLA$_{40}$, and g) PLA.

The FT-IR spectroscopy was used to identify the functional groups of the materials. The FTIR spectra of PLA, *m*PEI, and *m*PEI-PLLA$_n$ are shown in Figure 4.2. The *m*PEI shows a broad band at 3285, 2937-2818, and 1668 cm^{-1} which are attributed to hydrogen bonding in *m*PEI with H_2O, C-H stretching and NH_2 in primary amines, respectively. The FT-IR spectra of the PLA show a pack at 2995-2945, 1757, and 1383-1454 cm^{-1} which is attributed to C-H stretching, carbonyl, and

C-O-H bending. The FT-IR spectra of the *m*PEI-PLLA shows at 3306, 2990-2943, 1752, 1654, and 1611 cm^{-1} which is attributed to hydrogen bonding of hydrogen in *m*PEI with H_2O, C-H stretching, carbonyl, amide I (C=O stretch) and amide II (NH bending).

The structural characterization of *m*PEI-$PLLA_n$ was done by ^{1}H-NMR. The ^{1}H-NMR (chloroform-d) chemical shift at 4.38 ppm corresponds to methine shift (-COC**H**(CH_3)OH) due to the hydroxyl terminal of the PLLA unit, while a peak at 5.21 ppm corresponds to methine group (-COOC**H**(CH_3)-) in PLLA unit. A broad signal at 2.0-4.2 ppm, corresponds to the protons of *m*PEI core, whereas the sharp signals at 1.46 and 1.57 ppm refer to methyl protons of terminal group(-COCH(C**H**$_3$)OH), and main chain (-COOCH(C**H**$_3$)-) of PLLA, respectively (Appendix A (Figure A3)). When PLLA content in *m*PEI-PLLA was increased, the proton signal of *m*PEI gradually decreased and finally disappeared at 40:1 molar feed ratio. This implies it is important to note that PLLA chain was extended with increasing molar feed ratio which the proton signal of PLLA chain was intense obviously with the hidden proton signal of *m*PEI.

The *m*PEI-$PLLA_n$ was confirmed by ^{13}C-NMR (Appendix A (Figure A3)). The broad signal at 35.0-55.2 ppm corresponds to the carbons of *m*PEI core, and the signal at 69.9 ppm relates to the carbon of the methane group (-CO**C**H(CH_3)OH). The signal at 17.1 ppm is for the carbon of the methane group (**C**OCH(CH_3)OH), of end chain of PLLA . The chemical shifts of are interest at 175.51 and 170.05 ppm which correspond to amide bond (-NH**C**O(CH_3)-) and ester bond (-**C**OOCH(CH_3)-), respectively. This confirms that *m*PEI is able to open the *L*-lactide ring successfully.

Considering *m*PEI as a core molecule for PLLA arms, the degree of polymerization (DPn) of PLLA arms can be calculated from integral ratio of methane proton at main chain (5.21 ppm) and terminal group (4.38 ppm) as following eq. (4.1).

$$DPn = \frac{CH_{PLLA}}{CH_{PLLA\ end\ group}} \qquad (4.1)$$

The DPn obtained is an average number of PLLA repeating units in each arm on a core *m*PEI molecule.

Table 4.1 Average molecular might of *m*PEI-PLLA copolymers from NMR and GPC techniques

Entry	Molar feed ratio *m*PEI/*L*-LA	NMR		GPC		
		DPn[a]	M_n[b]	M_n[c]	M_w[d]	PDI[e]
1	1/166	3	1.7×10^4	9.86×10^3	1.24×10^4	1.26
2	1/415	5	2.8×10^4	1.02×10^3	1.30×10^4	1.27
3	1/581	7	3.9×10^4	1.09×10^4	1.37×10^4	1.26
4	1/830	10	5.6×10^4	1.17×10^4	1.38×10^4	1.17
5	1/1162	14	7.9×10^4	1.31×10^4	1.37×10^4	1.05
6	1/3320	40	2.2×10^5	1.53×10^4	2.41×10^4	1.57
7	1/6640	80	4.5×10^5	1.67×10^4	2.88×10^4	1.72

[a] Number-average degree of polymerization calculated from eq. (4.2).

[b] Number-average molecular weight determined by ^{1}H-NMR.

[c] Number-average molecular weight determined by GPC.

[d] Weight-average molecular weight determined by GPC.

[e] Polydispersity index measured by GPC.

$$Mn = 78(DPn \times 72)+72 \qquad (4.2)$$

*m*PEI-PLLA$_n$ denote the multi-arm star copolymer *m*PEI-PLLA; n means the average degree of polymerization of lactic acid units in the PLLA arms such as *m*PEI-PLLA$_3$, *m*PEI-PLLA$_5$, *m*PEI-PLLA$_7$, *m*PEI-PLLA$_{10}$, *m*PEI-PLLA$_{14}$, *m*PEI-*m*PLLA$_{40}$, PEI-PLLA$_{80}$.

Table 4.1 shows the average molecular weight of *m*PEI-PLLAs determined by NMR and GPC techniques. It is clear that number-average molecular weight (M_n) obtained is increased with increasing of *m*PEI/L-LA molar feed ratio.

This indicated that PLLA chain length in *m*PEI-PLLAs was controlled directly by L-LA molar feeding. Moreover, the average molecular weight of *m*PEI-PLLAs obtained from these two techniques are different because the determined molecular weights of multi-branched polymers from size exclusion chromatography are normally less than that of linear polymer at the same molecular weight. PDI values of all *m*PEI-PLLAs are in the range of 1.0 to 1.7, implying that PLLA polymerization and its chain length on each branch are almost identical.

4.4.2 Thermal Properties of *m*PEI-PLLA$_s$ Copolymers

In order to verify the role of *m*PEI-PLLAs as plasticizer for PLA, the thermal performances of PLA/*m*PEI-PLLA blends traced by DSC were applied. Non-isothermal crystallization studies allow us to follow the glass transition temperature (T_g) change of *m*PEI-PLLAs which strongly relates to PLA plasticity in the blend. Figure 4.3. shows the plot of T_g change of *m*PEI-PLLAs as a function of various PLLA-arm chain length of *m*PEI-PLLA.

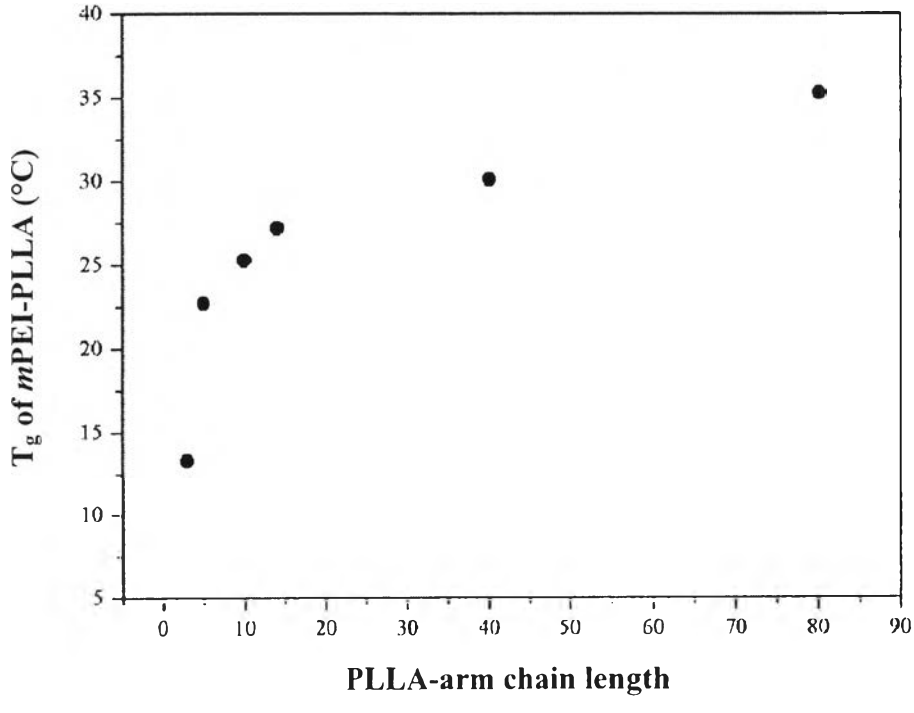

Figure 4.3 Glass transition temperature (T_g) of *m*PEI-PLLAs in various DPn with various PLLA-arm length.

In general, T_g of neat PLA and *m*PEI are 50-55°C and -52°C, respectively. In case of *m*PEI-PLLAs, only single T_g was observed and their T_g are lower than that of neat PLA but higher than neat *m*PEI. The decrease of their T_g is relevant to the length of branches which was demonstrated in Figure 4.3. The shorter *m*PEI-PLLAs (n=3-14 unit) provide the lower T_g which might be susceptible to heat and easily crystallized themselves as a consequence. From this phenomenon, these short *m*PEI-PLLAs considerately perform the potential in chain mobility enhancement of high molecular weight PLA (PLA resin) which efficiently assists and increase free volume in PLA. Regarding long *m*PEI-PLLAs branches (n=40-80 unit), they also show the similar possibility in PLA crystallization acceleration; however, their performances could be slower than the short *m*PEI-PLLAs, estimated from *m*PEI-PLLAs T_g.

4.4.3 Thermal Properties of PLA/*m*PEI-PLLA Blends

After PLA blended with *m*PEI by varying weight ratio (10-30%), two T_g appeared obviously as shown in Table 4.2. It indicated that phase separation between PLA and *m*PEI occurred. Meanwhile, amorphous *m*PEI induced the reduction of T_c and T_m of PLA, it could be noted that multi-branched structure increases free volume and enhances polymer chains mobility in the blend (Hassouna *et al.* (2011)). Whereas PLA blended with *m*PEI-PLLAs shows only single T_g, it implies that the miscibility between PLA and *m*PEI was improved significantly by applying *m*PEI-PLLAs copolymers.

From overall of T_g, T_c, and T_m of *m*PEI-PLLAs blends in various weight ratios, both T_g and T_c of PLA after blending with *m*PEI-PLLAs shift to lower temperature which affirm the important functions of *m*PEI-PLLAs in free volume expansion and chains mobility improvement. The T_g around room temperature suggests an increase in segmental mobility of the PLA chains. This allows rearranging and crystallization as reported by Hassouna *et al.* (2011). Nevertheless, T_g and T_m of PLA/*m*PEI-PLLAs blends slightly increase with PLLA chains length in *m*PEI-PLLAs due to the increment of PLLA chains content in blends.

Table 4.2 Glass transition (T_g), crystalline (T_c) and melting (T_m) temperature of PLA and it blends measured by DSC

Sample	T_g (°C)			T_c (°C)			T_m (°C)		
	Content of PEI-PLLA								
	10%	20%	30%	10%	20%	30%	10%	20%	30%
PLA/*m*PEI	9.9 39.7	10.5 37.9	15.2 36.2	97.9	101.8	99.6	134.5	132.8	126.0
PLA/*m*PEI-PLLA$_3$	41.4	40.3	39.7	99.6	99.9	97.0	147.6	147.5	132.6
PLA/*m*PEI-PLLA$_5$	41.5	39.8	39.1	111.4	105.6	104.4	146.8	145.4	144.6
PLA/*m*PEI-PLLA$_{10}$	43.9	43.4	42.2	116.0	115.2	111.4	149.5	148.5	146.8
PLA/*m*PEI-PLLA$_{14}$	45.8	41.3	40.3	115.9	113.4	111.5	152.6	147.4	146.6
PLA/*m*PEI-PLLA$_{40}$	46.6	46.5	43.4	110.4	108.3	100.7	151.9	155.8	151.2
PLA/*m*PEI-PLLA$_{80}$	45.6	37.5	45.5	109.0	92.4	105.1	153.0	147.7	156.2

* T_g, T_m, and T_c of PLA are 55, 113.1, and 153.9 °C, respectively.
T_g of PEI is -52 °C

The quantitative analysis for PLA crystallization improvement by using *m*PEI-PLLAs as both nucleating agent and plasticizer was further investigated. Degree of crystallinity (X_c) was calculated by comparing the melting enthalpy change of our blends (ΔH_m) to the fusion heat of fully crystallized PLA (ΔH^0_m) 93.1 J g^{-1} (Sarasua *et al.*, 1998; Ouchi *et al.*, 2006; Kawamoto *et al.*, 2007; Liao *et al.*, 2007). The crystallinity of PLA blended with *m*PEI, decreases with increases of *m*PEI contents in the blend which might be due to high amorphous *m*PEI, as tabulated in Table 4.3. This declined crystallinity of PLA is evident that multi-branches *m*PEI structure and phase separation in PLA/*m*PEI blend obstruct of PLA packing.

Table 4.3 Enthalpy changes of crystallization (ΔH_c) and melting (ΔH_m) and degree of crystallinity (X_c), obtained from the 2nd DSC scan

Sample	ΔH_c[a] (J/g)			ΔH_m[b] (J/g)			X_c[c] (%)		
	Content of PEI-PLLA								
	10%	20%	30%	10%	20%	30%	10%	20%	30%
PLA/*m*PEI	16.75	7.68	0.43	17.88	9.62	1.00	21.12	12.40	1.40
PLA/*m*PEI-PLLA$_3$	17.43	22.38	20.08	21.01	26.08	23.72	24.83	33.62	33.12
PLA/*m*PEI-PLLA$_5$	29.59	26.70	23.51	31.58	30.35	26.91	37.32	39.12	37.58
PLA/*m*PEI-PLLA$_{10}$	13.32	12.40	11.72	17.18	14.63	15.97	20.30	18.86	22.30
PLA/*m*PEI-PLLA$_{14}$	21.22	7.12	11.47	29.28	12.70	13.82	34.60	16.37	19.30
PLA/*m*PEI-PLLA$_{40}$	31.34	31.06	27.58	33.09	36.43	35.48	31.11	35.70	32.66
PLA/*m*PEI-PLLA$_{80}$	33.10	29.33	33.43	34.10	39.96	39.69	33.25	37.43	34.31

* ΔH_c, ΔH_m, and X_c of PLA are 19.66 J/g, 28.32 J/g, and 30.45%.

[a,b] calculated from areas under T_c and T_m peaks

[c] calculated from X_c = (ΔH_m x 100)/(93.1 x PLA weight fraction)

Tendencies of increased ΔH_m, ΔH_c, and X_c of all blends with 10% *m*PEI-PLLAs are similar, they were rose with PLLA-arm chains length, excepting for *m*PEI-PLLA10. Anyhow, the X_c of PLA was remained even the contents of *m*PEI-PLLAs in each blend were increased from 10% to 30%.

4.4.4 Morphology of PLA/*m*PEI-PLLAs Blend Films

The miscibility between PLA and *m*PEI-PLLAs was followed by SEM images (Figure 4.4).

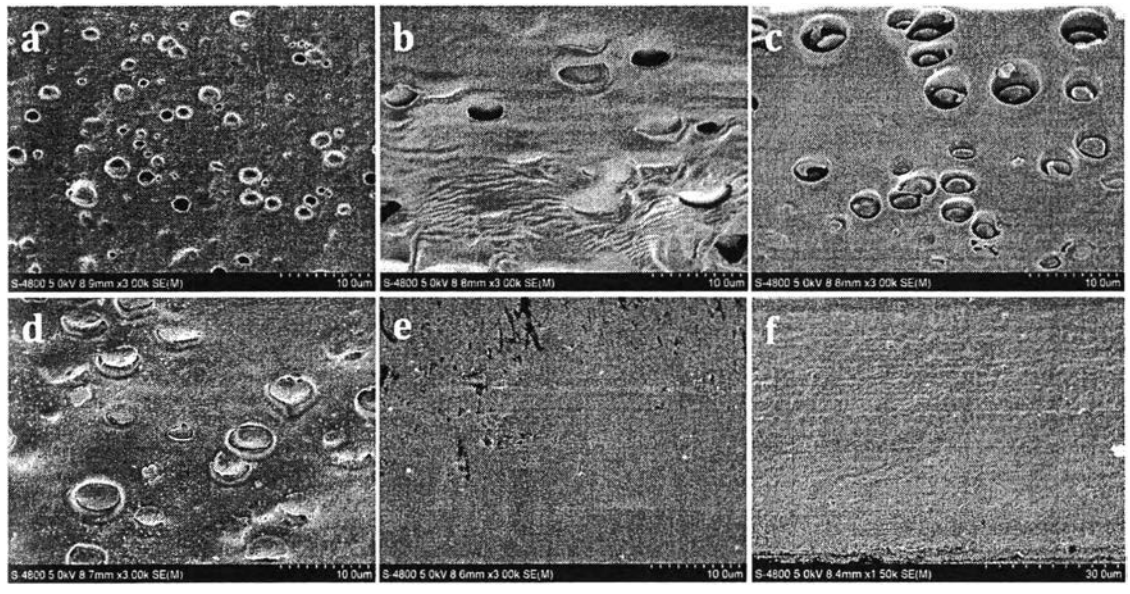

Figure 4.4 SEM micrographs of PLA/*m*PEI-PLLAs 90/10 blend films; a) *m*PEI-$PLLA_3$, b) *m*PEI-$PLLA_5$, c) *m*PEI-$PLLA_{10}$, d) *m*PEI-$PLLA_{14}$, e) *m*PEI-$PLLA_{40}$ and f) *m*PEI-$PLLA_{80}$.

Due to degradation of *m*PEI at high temperature, PLA/*m*PEI blend film cannot be characterized when it was coated with platinum. In case of short PLLA-arm in *m*PEI-PLLAs, PLA/*m*PEI-$PLLA_3$ surface shows some voids whose size was increased with PLLA chain length (n = 5 and 10). The average size of voids increased from about 3 μm to 5 μm and agglomeration of *m*PEI-$PLLA_n$ particles was observed which may affect the mechanical properties of the blend films. However, when the PLLA-arm length was extended to n = 14, the void size was clearly decreased. Finally, the voids can be diminished completely by rising of PLLA chains length at 40 and 80 L-LA units. This miscibility improvement performs an agreement with the single T_g as observed from DSC scan.

4.4.5 Effects of *m*PEI-$PLLA_n$ on PLA Spherulite Formation in Blends

The crystallization behaviors of blend commercial PLA with *m*PEI-$PLLA_n$ were studied by optical microscope.

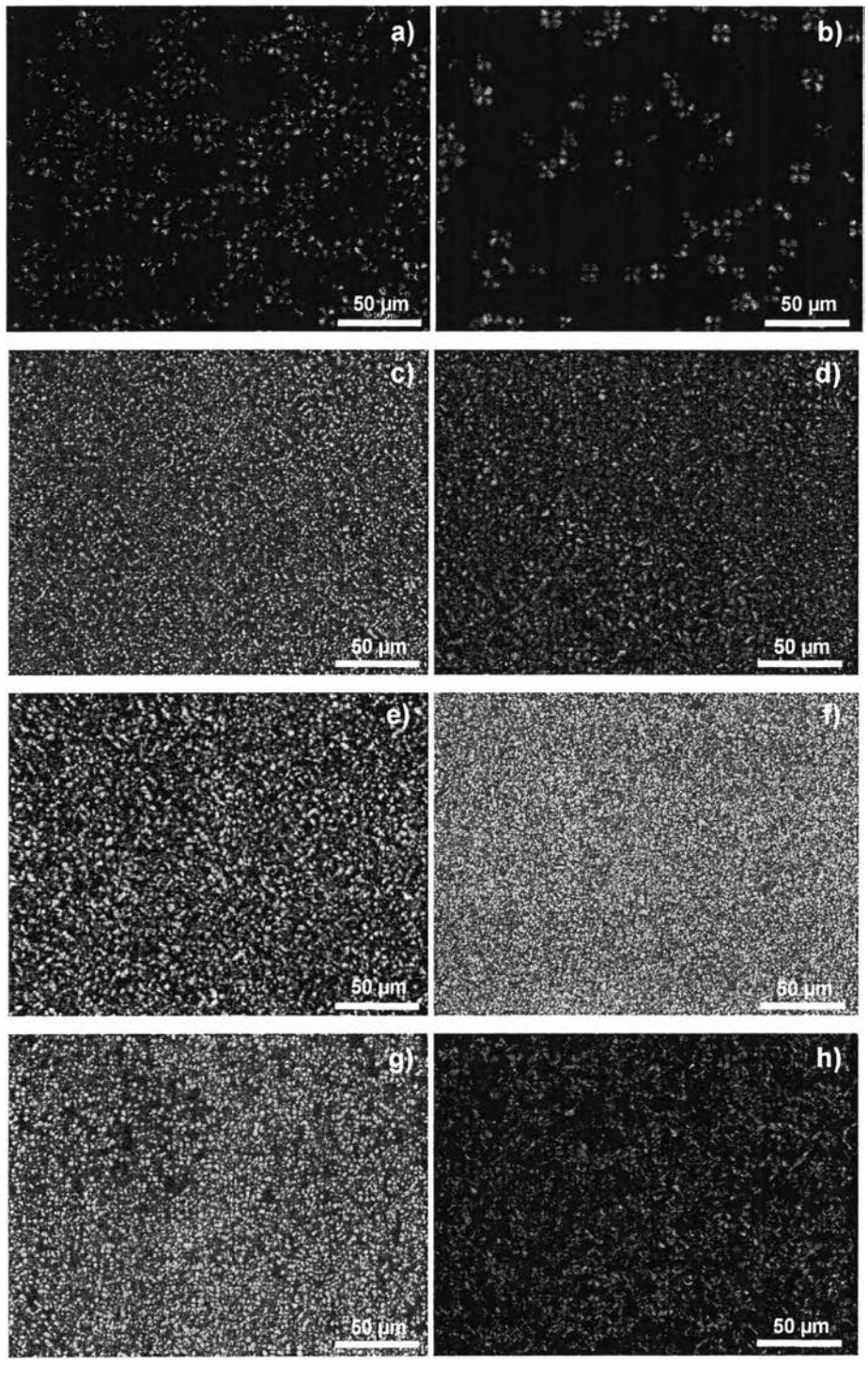

Figure 4.5 Optical micrographs of a) PLA and PLA/*m*PEI-PLLAs blends with varied weight ratios at 110 °C: b) PLA/*m*PEI-$PLLA_3$ 10%, c) PLA/*m*PEI-$PLLA_3$ 20%, d) PLA/*m*PEI-$PLLA_3$ 30%, e) PLA/*m*PEI-$PLLA_5$ 20%, f) PLA/*m*PEI-$PLLA_{14}$ 20%, g) PLA/*m*PEI-$PLLA_{40}$ 20 %, and h) PLA/*m*PEI-$PLLA_{80}$ 20 %

The isothermal crystallization was also studied in order to follow crystallization behavior of PLA after blending with *m*PEI-PLLAs. Under polarizing optical microscope observation at 110 °C, we found that the spherulite size of PLA drastically decreased when PLA blended with *m*PEI-PLLA3 20% (Figure 4.5a-h). The density of spherulite formation of all PLA/*m*PEI-PLLAs blends was enhanced successfully, compared to that of pure PLA, especially *m*PEI-PLLAs with $n \leq 40$. It is worth mentioning that *m*PEI-PLLAs copolymers effectively function as nucleating agent for PLA.

4.4.6 Mechanical Properties of *m*PEI-PLLAs/PLA Blend Films

Regarding of mechanical properties of PLA blended with *m*PEI-PLLAs films in Figure 4.6.

20% *m*PEI-PLLAs blends marvelously improved the PLA flexibility, the percentage of elongation at break of those blends was drastically raised from ~6 % to ~280 %. 20% *m*PEI-PLLA$_{10}$ blend demonstrated the highest flexibility due to relatively short PLLA chains length. In its system, there were both crystalline and amorphous phases which can increase crystallization and free volume sufficiently. Blended films can be stretched under an influence of PLLA-arm chains length. *m*PEI-PLLAs with high PLLA-arm chains length (40 and 80 L-LA units) contributed to low percentage of elongation at break. In case of 30% *m*PEI-PLLAs blends, elongation at break was suddenly dropped down. This can be ascribed as a good dispersion of *m*PEI-PLLA$_n$ in PLA matrix occurred at *m*PEI-PLLA$_n$ content less than 20. Tensile strength of blends films decreased with *m*PEI-PLLAs contents which could be an effect of free volume increment in the system.

It is worth considering that the PLA flexibility enhancement can be achievable by optimizing of crystalline and amorphous phases with high crystallization rate in the system. Additionally, the use of multi-branched PLLA is an efficient way to improve the mechanical properties of PLA as the results of not only the enhanced crystallization but also the partial-miscibility in the blends.

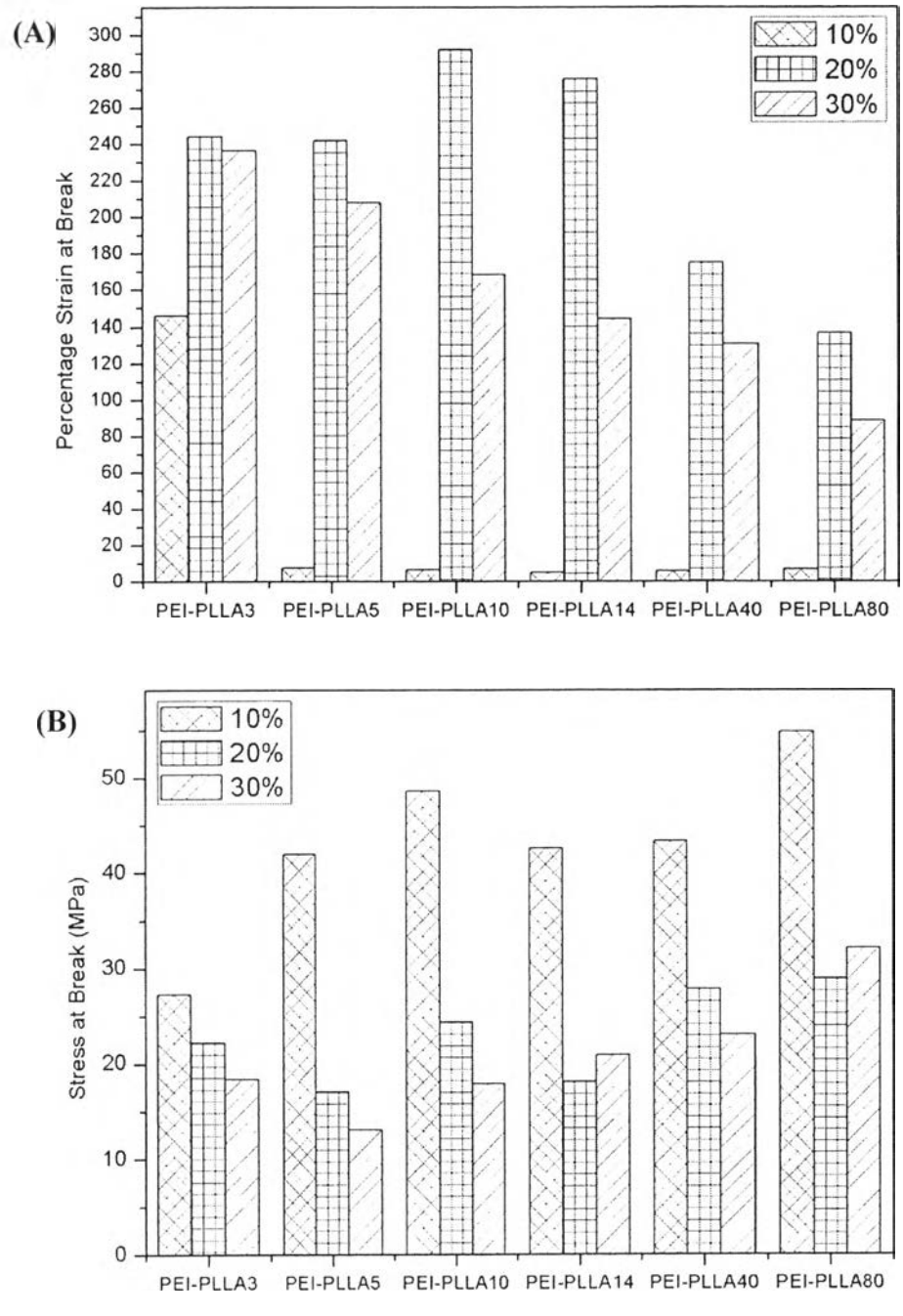

Figure 4.6 Mechanical properties of PLA/*m*PEI-PLLA$_n$ (A) tensile strength, and (B) elongation at break

4.5 Conclusions

*m*PEI-PLLAs copolymers were successfully synthesized by ring-opening polymerization of L-LA with PEI. The PLLA-arm chains length connected with core PEI molecules was determined by quantitative analysis from ^{1}H-NMR spectra. The T_g of *m*PEI-PLLAs increased with increasing of PLLA-arm chains length. After PLA/*m*PEI-PLLAs blending, PLA T_g of the blends was declined whereas their crystallization of PLA was improved, verified by increment of PLA crystallinity and spherulite density. The present work shows that *m*PEI-PLLA simultaneously acts as both nucleating agent and plasticizer to enhance PLA crystallization rate. Not only PLA crystallization acceleration but also miscibility in blends were accomplished by adding *m*PEI-PLLAs in the system, resulting in PLA flexibility enhancement obviously which was based on optimizing crystalline and amorphous phases in the system.

4.6 Acknowledgements

The authors gratefully acknowledge Junior Science Talent Project (JSTP) No. JSTP-06-54-05E, National Science and Technology Development Agency (NSTDA) and the Petroleum and Petrochemical College; and the National Center of Excellence for Petroleum, Petrochemicals, and Advanced Materials, Thailand.

4.7 References

Cai, J., Liu, M., Wang, L., Yao, K., Li, S. and Xiong, H. (2011) Isothermal crystallization kinetics of thermoplastic starch/poly(lactic acid) composites. Carbohydrate Polymers, 86(2), 941-947.

Chivrac, F., Kadlecova, Z., Pollet, E. and Averous, L. (2006) Aromatic Copolyester-based Nano-biocomposites: Elaboration, Structural Characterization and Properties. Journal of Polymers and the Environment, 14, 393-401.

Hassouna, F., Raquez, J.-M., Addiego, F., Dubois, P., Toniazzo, V. and Ruch, D. (2011) New approach on the development of plasticized polylactide (PLA):

Grafting of poly(ethylene glycol) (PEG) via reactive extrusion. European Polymer Journal, 47(11), 2134-2144.

Hu, Y., Rogunova, M., Topolkaraev, V., Hiltner, A. and Baer, E. (2003) Aging of poly(lactide)/poly(ethylene glycol) blends. Part 1. Poly(lactide) with low stereoregularity. Polymer, 44(19), 5701-5710.

Kim, S., Shin, K., Lee, S., Kim, K. and Youn, J. (2010) Unique crystallization behavior of multi-walled carbon nanotube filled poly(lactic acid). Fibers and Polymers, 11(7), 1018-1023.

Li, H. and Huneault, M.A. (2007) Effect of nucleation and plasticization on the crystallization of poly(lactic acid). Polymer, 48(23), 6855-6866.

Li, H. and Huneault, M.A. (2011) Comparison of sorbitol and glycerol as plasticizers for thermoplastic starch in TPS/PLA blends. Journal of Applied Polymer Science, 119(4), 2439-2448.

Ljungberg, N. and Wesslén, B. (2005) Preparation and Properties of Plasticized Poly(lactic acid) Films. Biomacromolecules, 6(3), 1789-1796.

Pangon, A., Tashiro, K. and Chirachanchai, S. (2011) Polyethylenimine Containing Benzimidazole Branching: A Model System Providing a Balance of Hydrogen Bond Network or Chain Mobility Enhances Proton Conductivity. The Journal of Physical Chemistry B, 115(39), 11359-11367.

Pillin, I., Montrelay, N. and Grohens, Y. (2006) Thermo-mechanical characterization of plasticized PLA: Is the miscibility the only significant factor? Polymer, 47(13), 4676-4682.

Sobkowicz, M.J., Dorgan, J.R., Gneshin, K.W., Herring, A.M. and McKinnon, J.T. (2008) Renewable Cellulose Derived Carbon Nanospheres as Nucleating Agents for Polylactide and Polypropylene. Journal of Polymers and the Environment, 16, 131-140.

Suksut, B. and Deeprasertkul, C. (2011) Effect of Nucleating Agents on Physical Properties of Poly(lactic acid) and Its Blend with Natural Rubber. Journal of Polymers and the Environment, 19, 288-296.

Suryanegara, L., Nakagaito, A.N. and Yano, H. (2010) Thermo-mechanical properties of microfibrillated cellulose-reinforced partially crystallized PLA composites. Cellulose, 17, 771-778.

Tsuji, H. and Muramatsu, H. (2001) Blends of aliphatic polyesters. IV. Morphology, swelling behavior, and surface and bulk properties of blends from hydrophobic poly(L-lactide) and hydrophilic poly(vinyl alcohol). Journal of Applied Polymer Science, 81(9), 2151-2160.